UNIVERSITAT POLITÈCNICA DE CATALUNYA
BARCELONATECH
Escola d'Enginyeria de Telecomunicació
i Aeroespacial de Castelldefels

TREBALL DE FI DE GRAU

TFG TITLE: Potential flow of perfect fluids on complex surfaces

DEGREE: Grau en Enginyeria d'Aeronavegació

AUTHOR: Alba Martín Muñoz

ADVISORS: Pietro Alberto Massignan
Santiago Torres

DATE: July 6, 2018

Títol: Fluxe potencial de fluids perfectes en superfícies complexes

Autor: Alba Martín Muñoz

Directors: Pietro Alberto Massignan
Santiago Torres

Data: 6 de juliol de 2018

Resum

Aquest document estudia el comportament dels fluids perfectes al passar per diferents superfícies històricament utilitzades per al disseny de perfils d'ala. A més d'això, alguns potencials de fluids es representen sobre superfícies tridimensionals realitzades amb projeccions del pla complex inicial. En comptes de dur a terme un desenvolupament numéric, en aquest estudi es segueix una estrategia completament analitica, basada en la teoria dels potencials complexes i transformacions conformes. Per visualitzar els resultats hem desenvolupat codis basats en el sotfware Wolfram Mathematica. L'anàlisi així obtinguda, proporciona un enfocament analític que pot ser una alternativa als mètodes de simulació numèrica o, en alguns casos, ambdues estratègies també poden ser complementàries..

Title : Potential flow of perfect fluids on complex surfaces

Author: Alba Martín Muñoz

Advisors: Pietro Alberto Massignan
Santiago Torres

Date: July 6, 2018

Overview

This document studies the behavior of perfect fluids when passing around different surfaces that have been historically used for the design of wing profiles. In addition to that, some fluid potentials are represented over three-dimensional surfaces performed with projections of the initial complex plane. Rather than taking a numerical approach, we follow here a completely analytical strategy, based on the theory of complex potentials and conformal transformations. In order to visualize the results we developed specific pieces of code based on the Wolfram Mathematica sotfware. The analysis thus obtained provides an analytical approach that can be an alternative to numerical simulation methods, or for some cases both strategies can also be complementary.

A la meva mare
Per haver-me donat suport en tot moment i pels seus consells.

Al meu pare
Per haver-me ensenyat que amb cura i paciència tot és possible.

A la meva parella
Per no deixar anar la meva mà mai i per l'amor incondicional.

CONTENTS

LIST OF FIGURES

ACKNOWLEDGMENT

Després de tants mesos treballant en aquest projecte, es el dia d'escriure els agraïments per tal de concloure amb aquesta etapa. Ha sigut un període d'aprenentatge intens, no solament en el camp ciéntific sino també al personal.

Primerament, m'agradaria donar les gràcies al meu tutor *Pietro Massignan* per haver-me donat la oportunitat de fer el treball amb ell. Encara recordo el primer dia, quan no teníem clar per on agafar aquest embolic, vam agafar diferents camins fins que a la fí vam donar amb un tema que ens agradava als dos. Has estat molt pacient amb mi i m'has ensenyat a pensar d'una manera nova, més crítica, amb una ment una mica més semblant a la d'una física.

D'altra banda, agrair al meu altre tutor *Santiago Torres* per ser el guia d'aquesta experiència i haver posat ordre tant a la feina com en els procediments necessaris per que tot sortís bé, gràcies pels teus consells.

Finalment, donar el meu agraïment de tot cor al meus familiars i a la meva parella per haver aguantat el meu mal humor quan no hem sortien les coses com jo volia i quan no els hi feia molt de cas per que estava treballant en aquest projecte. Gràcies per animar-me a seguir endavant sempre i per el vostre amor incondicional.

A tots vosaltres el meu major reconeixement i gratitud.

INTRODUCTION

Motivation

Serious airfoil design began in the late 19th century. It was already known that flat plates under some angle of attack were capable to produce lift force but it was also observed that shapes with curvature, more closely resembling bird wings, would produce even more lift.

Testing each airfoil design at that epoch required to create wind tunnels with artificial currents of air that could not achieve high values of Reynolds number. Later on, aerodynamic research has been carried out in increasingly sophisticated environments, with sensors for each of the necessary data and carried out in different situations in both subsonic and supersonic conditions.

Nowadays, wind tunnel testing demand has been reduced due to the advances done in Computational Fluid Dynamics (CFD). Based on numerical analysis and data structures, this branch of Aerodynamics solves problems involving many types of fluids flows. The numerical solution is very demanding, so that high speed supercomputers are often needed. On the other hand, so-called perfect fluids (which are incompressible and inviscid) admit a completely analytical description in terms of potentials in the complex plane. This alternative method can be very powerful, and in this TFG we will see various interesting applications of it.

General approach and Objectives

This research has been based on complex potential theory in addition with conformal mapping techniques. Making an analytic resolution of fluids flow with the objective of analyzing it on complex surfaces has led to the necessity of well understanding mathematical transformations from one plane to another.

The main objectives of this work may be summarized as follow:

1. Study the physics describing perfect fluids.
2. Introduce the theory of complex potentials and conformal mappings.
3. Apply these advanced mathematical techniques to the solution of perfect fluid flow in a series of realistic situations.

The tool used for generating the plots is the “Wolfram Mathematica” software. This system for modern technical computing covers all areas of computing. With plenty of integrated functions and algorithms it is capable of presenting interactive visualizations and illustrative figures.

Document structure

The document is written in such a way that the knowledge can be acquired by the reader in a smooth way, first introducing the basic notions, then the mathematical theory, and finally applying the methods to study a series of concrete cases.

This *Chapter* gives a brief introduction. In *Chapter 1* the most basic concepts of fluids are introduced. Starting with the description of some of their properties and explaining the different types that exist, one arrives at what is really the focus of this study: perfect fluids. Here also basic dynamics and complex potentials are developed. Then in *Chapter 2* conformal maps are developed with the aim of being able to represent fluid flow on a variety of different surfaces. In *Chapter 3* complex potentials are combined with conformal mappings to describe flow around surfaces like cylinders, ellipses, flat plates and Joukowski wings. A naive application of these methods often generates flows with unrealistic features. In *Chapter 4* it is discussed how to fix this problem, by taking into account the so-called Kutta condition, and the resulting pressure distributions and lift are calculated. To conclude, in *Chapter 5* the methods of complex potentials are applied to describe fluid flow on a variety of 3D surfaces.

CHAPTER 1. FLUID MECHANICS. BASIC NOTIONS

A fluid is substance having the property of flowing without rigidity and elasticity, and consequently yielding to any force acting on it. The state variables of the material can be considered continuous functions of space and time, leading to the description of the material as a continuous medium. Therefore, when speaking about a fluid one generally considers a volume element containing a very large number of molecules.[1]

One of the most striking characteristic of fluids is the absence of shape memory. This defining property is possible thanks to the absence of reconstructive forces tending to keep its original shape that, for instance, are present in deformable solids. Molecules in a fluid move around and slide past one another, but are still attracted to one another through inter molecular forces of attraction. Given that the molecules have not an equilibrium position they can move as much as necessary so the fluid can flow as desired.[2]

Liquids and gases are both fluids. Liquids normally flow from higher levels to lower ones but gases flow in random directions determined by external factors. When a gas is introduced in a container it fills the whole volume whereas liquids have a surface tension and therefore develop a free surface (that is, a surface not created by the container) always with a fixed volume.

The behaviour of fluids is determined by a series of continuous variables, such as, density, temperature and pressure. Density quantifies the ratio of mass per unit volume, temperature determines the amount of kinetic energy of the microscopic components of the fluid, and pressure is the ratio of force on a fluid to the area held perpendicular to the force. Other relevant properties are the specific volume which measures the volume occupied per unit mass, and the specific weight which is the weight per unit volume of a fluid.

Two other important properties that are relevant for hydrodynamic analysis: compressibility and viscosity. It is worthy to stop and correctly understand the concepts, that are explained as follows:

- **Compressibility** quantifies how easily the volume V of a body changes when its subject to a pressure p:

$$\beta = -\frac{1}{V}\frac{\partial V}{\partial p} \tag{1.1}$$

In the case of gases, molecules are widely separated so they are highly compressible but for liquids the separation is not that wide so cannot be very compressible.

- **Viscosity** is the property that measures how can the deformation velocity increases inside a fluid. It is present in all types of fluids (smaller in gases) due to the continuous deformation they suffer under shear stresses. The collision between the fluid particles that move at different layers causes the resistance to movement. It is governed by Newton's law of viscosity, that states that

$$\tau = \mu \frac{\partial u}{\partial y}, \tag{1.2}$$

where τ is the shear stress, μ is the viscosity and $\partial u/\partial y$ is the rate of shear deformation.

1.1. Type of fluids

Usual fluids are compressible, so they change their volume when a force is applied. On the contrary, the volume of an incompressible fluid remains unaltered under pressure changes, and so does the density. Normally liquids tend to be little compressible, while gases are highly compressible. Even though, there are many realistic situations in which the density of a gas remains sufficiently constant as to consider it incompressible.

Tangential stresses inside gases are generally very small, while they may be important in certain fluids, leading to a non-negligible viscosity. It is worth noticing morever that viscosity is highly dependant on the fluid's temperature. Maple syrup, for example, is very sticky when inside the bottle, but it becomes more watery when it is scattered on a hot waffle.

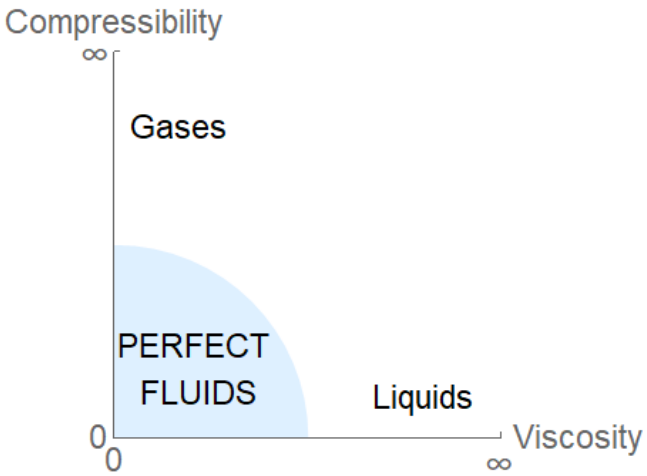

Figure 1.1: Fluids classification depending on viscosity and compressibility.

Real fluids deform continuously for a certain amount of shear stress and are capable to change their volume for a certain pressure (viscid and compressible). Some examples are: water, oil and glycerine.

Ideal or *perfect* fluids can flow without any stress on them, and do not change its volume under pressure (inviscid and incompressible). Some examples are: dry water (neglecting viscosity), Bose-Einstein condensates (a state of matter in which extremely cold atoms clump together and act as if they were a single atom) and Quark-Gluon plasmas (state of matter studied in quantum chromodynamics, which is found at extremely high temperature or density).

1.1.1. Perfect fluids

A fluid is said to be *ideal* or *perfect* if both its viscosity and its compressibility are negligible. Although these seem to be rather extreme approximations, both air and water may often be treated as ideal fluids. Indeed, both these fluids have very little viscosity. Moreover, compressibility in a fluid generally becomes noticeable only when the fluid speed v approaches the sound speed c. Sound travels in air at ~ 300m/s, and in water it travels 4 times faster

than that. As a rule of thumb, we may consider a fluid incompressible whenever $v < 0.3c$. Therefore, many realistic flows may be described as ideal.

1.2. Dynamics of perfect fluids

Fluid dynamics aims at describing the flow of fluids in response to external forces, and the forces that fluids exert on surrounding bodies. Solving a fluid dynamics problem involves the computation of different fluid properties as flow velocity, temperature, density and pressure as function of time and space.

In order to describe the motion of a fluid it is necessary to know its properties at every point in space and time. In this case it will be assumed that density is a constant (incompressible fluid). By making this hypothesis it is assumed that the variations of density are so small that can be neglected $\delta\rho = 0$, thus the fluid can be considered incompressible without making a big error.[3]

It is necessary now to consider the conservation of matter. If the fluid velocity is $\vec{v}$, then the mass which flows in a unit time across a unit area of surface is the component of $\rho\vec{v}$ normal to the surface, and the continuity equation can be written as

$$\frac{\mathrm{d}\rho}{\mathrm{d}t} + \nabla \cdot (\rho\vec{v}) = 0 \tag{1.3}$$

In the case of present interest, of a steady and incompressible flow, the continuity equation can be reduced to

$$\nabla \cdot \vec{v} = 0 \tag{1.4}$$

The circulation around any closed path in a fluid is the line integral of the fluid velocity at a given time around that path. Using the Green-Stokes Theorem, one may write this quantity in terms of the curl of the velocity

$$k = \oint_c \mathrm{d}\vec{l} \cdot \vec{v} = -\int\int \mathrm{d}\vec{s} \cdot (\nabla \times \vec{v}) \tag{1.5}$$

If the fluid on top of being incompressible is also irrotational, then (1.5) is zero and there exists a velocity potential such that

$$\vec{v} = \nabla\Phi \tag{1.6}$$

For a steady, incompressible and irrotational flow in two dimensions, it can be demonstrated that there exists also a stream function Ψ which represent the trajectories of particles in a steady flow. Both these functions are called “harmonic” because they fulfill the so-called Laplace equation

$$\nabla^2\Phi = 0, \qquad \nabla^2\Psi = 0 \tag{1.7}$$

Introduced by the physicist and mathematician Pierre-Simon Laplace [13], this equation applies not only to hydrodynamics, but actually describes a great variety of problems such as electrostatics, diffusion, and membrane stretching. Understanding it in some simple cases is a great help when one wants to understand behaviors of more complicated equations.

1.3. Complex potential Theory

For a 2D incompressible and irrotational flow, the velocity field $\vec{v} = \{u, v\}$ can be expressed in terms of Φ and Ψ as

$$u = \frac{\partial \Psi}{\partial y} \qquad v = -\frac{\partial \Psi}{\partial x} \qquad\qquad u = \frac{\partial \Phi}{\partial x} \qquad v = \frac{\partial \Phi}{\partial y} \tag{1.8}$$

Using the irrotational condition and the continuity equation, one directly finds

$$\frac{\partial \Psi}{\partial y} = -\frac{\partial \Phi}{\partial x} \qquad \text{and} \qquad \frac{\partial \Psi}{\partial x} = \frac{\partial \Phi}{\partial y}. \tag{1.9}$$

If the two real functions Φ and Ψ are interpreted as the real and the imaginary parts of a complex function $F : \mathbb{Z} \to \mathbb{Z}$,

$$F(z) = \Psi(z) + i\Phi(z), \tag{1.10}$$

with $z = x + iy = re^{i\theta}$, one can recognize that the expressions in Eq. (1.9) are exactly the so-called *Cauchy-Riemann conditions* which ensure that $F(z)$ is an *analytic function*, i.e., it is "complex-differentiable" at every point within its domain, and its Taylor series also converges everywhere within the domain.

Vice-versa, it can also be shown that given *any* analytic function, both its real and imaginary parts are *always* solutions of the Laplace equation (1.7). Therefore, the real part and the imaginary part of any given analytic function F may always be interpreted as the stream function Ψ and the velocity potential Φ of a physical flow. In the rest of this work, we will therefore only consider analytical function F, and we will refer to them as "complex potentials".

Using the property of complex differentiation

$$\partial_z = \frac{1}{2}\left(\partial_x - i\partial_y\right), \tag{1.11}$$

one immediately finds that

$$\frac{\mathrm{d}F}{\mathrm{d}z} = \frac{1}{2}\left(\partial_x \Psi + i\partial_x \Phi - i\partial_y \Phi + \partial_y \Phi\right) = v_y + iv_x, \tag{1.12}$$

i.e., that the velocity components are straightforwardly obtained by complex differentiation of the complex potential. The velocity field will be very useful when requiring both the direction and magnitude of the velocity at any point of the space studied. Stagnation points and other singularities can be found thanks to this simple equation that once having the complex potential will just require its derivative.

To conclude, let us note that a linear combination of analytic functions is still an analytic function, so that it will keep solving Laplace equation (1.7). The same holds for the composition $G[F(z)]$ of two analytic functions F and G. This fact will be very useful when trying to solve more complicated configurations where more than one basic flow pattern will be needed to be applied.

CHAPTER 2. CONFORMAL TRANSFORMATIONS

Conformal transformations are functions M which map a surface to another, by conserving angles (locally) and orientations. A classic example is the map of the Earth that enlarges some countries and shrinks others in order to preserve angles.

An important property of conformal maps which plays a key role in this work is that if a function F is harmonic (i.e., a solution of Laplace's equation) over a certain domain, then its conformal image $F(M)$ will also be harmonic.

Understanding the flow of perfect fluids requires to find a solution to Laplace Equation (1.7) which can be reduced to finding an analytic function satisfying certain boundary conditions. Usually, if the domain is complicated this is done numerically, what sometimes leads to unreliable results. Here is where it comes conformal mapping, by using a suitable function $w = f(z)$ the problem is simplified thus conformal functions become very useful.[4]

The mapping function also converts an entire flow field around an initial surface into the flow field around any other surface. Then, by knowing velocities and pressures in the plane containing the initial surface the mapping function would give the velocity and pressure around the surface in the new plane. Some types of conformal transformations are explained in the next section.

2.1. Exponential and trigonometric mapping

Both exponential and trigonometric mapping try to simplify configurations in which the flow is enclosed by some walls (channel-shaped regions) by transforming them into a one simple wall. This type of maps may be very interesting in physical studies of the effects produced on a flow depending on the shape of the channel they cross through, but not for the purpose of this research.

- **Exponential maps** map channel-shaped regions into the half-space of the new plane. The complex function $\zeta = g(z) = e^{\pi z/h}$ drives the mapping from the channel of width h to the positive imaginary half-plane.

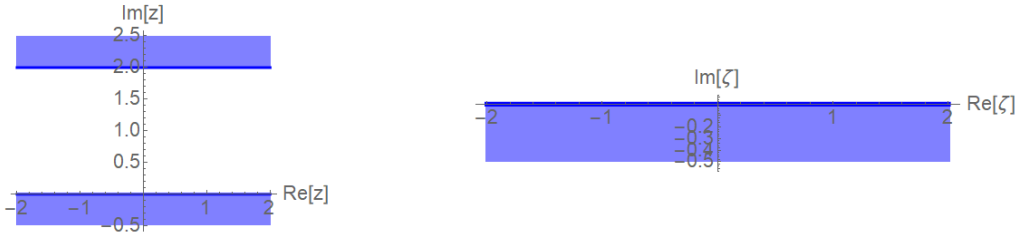

Figure 2.1: Left panel: Channel on $z - plane$. Right panel: Half-plane on $\zeta - plane$

The channel on the left side of *Figure 2.1* has now become a half-plane that would have a new analytic function describing the same flow pattern in the $\zeta - plane$.

- **Trigonometric maps** map a semi-infinite channel of width a into a half-space of the new plane. The effect of this mapping comes on the opening suffered on the corners of the channel that transform into a straight line. In this case the mapping corresponds to $\zeta = g(z) = \sin(z\pi/2a)$, where $\mathrm{Im}[z] > 0$ and $-a < \mathrm{Re}[z] < a$.

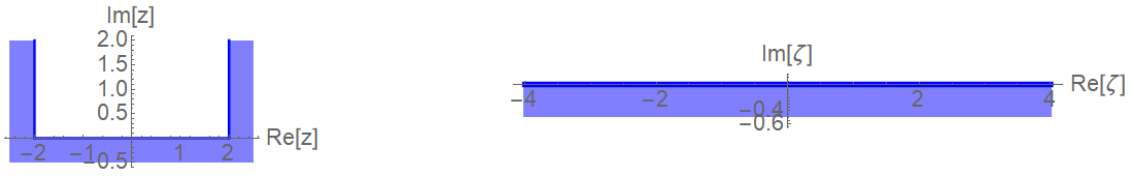

Figure 2.2: Left panel: U-shaped channel ($z-plane$). Right panel: Half-plane ($\zeta-plane$)

Just to make a concrete example, the point $z = 3i$ inside the channel is mapped onto the point $\zeta = isin(3\pi/2)$, which lies in the upper-half of the complex plane.

2.2. Wedges mapping

Another possibility of conformal mapping is the representation of a fluid inside a wedge. The transformation

$$\zeta = g(z) = z^{\pi/\alpha}, \tag{2.1}$$

maps a wedge of angular aperture α to the upper-half of the complex plane.

Let illustrate the utility of this with another concrete example. By means of the method of images, the potential for a vortex at position ζ_0 in the upper-half of the complex plane (i.e., delimited by a hard wall along the x-axis) is given by

$$F(\zeta) = \frac{Q}{2\pi}\log(\zeta - \zeta_0) - \frac{Q}{2\pi}\log(\zeta - \overline{\zeta_0}) \tag{2.2}$$

Combining the complex potential with the conformal map, one immediately obtains the complex potential for a vortex inside the wedge, which reads

$$W(\zeta) = \frac{Q}{2\pi}\log(\zeta - c^{\pi/\alpha}) - \frac{Q}{2\pi}\log(\zeta - \bar{c}^{\pi/\alpha}) \tag{2.3}$$

By representing the real part of the complex function $W(\zeta) = W\left((x+iy)^{\pi/\alpha}\right)$ it can be seen (in left panel of *Figure 2.3*) how would the stream lines be distributed if two walls were containing a vortex of strength Q. If there were no walls, the vortex would create constant stream lines for constant distance r measured from its origin but as the walls are close to the sides, here the stream lines flatten.

About the velocity field (in right panel of *Figure 2.3*), it is shown the rotating sense of the vortex that is anti-clock-wise in this case. As the distance from the center increases, the velocity decreases since its magnitude is inversely proportional to the radius.

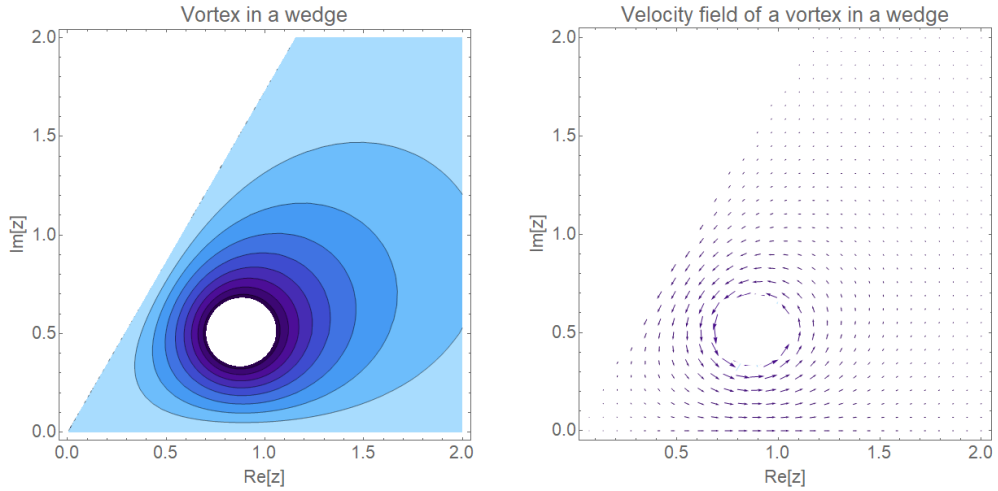

Figure 2.3: Vortex located at $z = c^{\pi/\alpha} = e^{i\,\alpha/2}$. Left panel: Stream function. Right panel: Velocity field.

2.3. Joukowski transformation

Joukowski transform is a type of conformal map historically used to understand airfoil design. The main idea of the transformation is to find a given flow in a region $R \subset \mathbb{C}$ that can be solved in an 'easier' way than it would normally be.[4]

To do so, it is first necessary to understand what is an holomorphic function. An holomorphic function (also known as analytic function) is a complex function that is said to be differentiable on every point in a specific region. A complex function may fail to be analytic at one or more points through the presence of singularities, or along lines or line segments known as branch cuts.[7]

The mapping consists on finding an holomorphic function $\zeta = g(z)$ so that the region R in the $z-plane$ is mapped to a much simpler region $\hat{R}$ in the $\zeta-plane$. Once transformed, the problem can be solved obtaining the complex potential $W(\zeta)$ and then it is only necessary to invert the mapping into the original $z-plane$.

The Joukowski transformation from the complex $\zeta-plane$ to the $z-plane$ is defined as

$$z = G(\zeta) = \zeta + \frac{a^2}{\zeta}, \tag{2.4}$$

where a is a real parameter which will be set to 1 unless specified and $\zeta = \chi + i\mu$, χ and μ being the complex coordinates in the $\zeta-plane$. This mapping is conformal except for $\zeta = 0$ (pole) and $\zeta = \pm 1$. Between those poles there is a branch cut, where the transformation develops very bizarre properties. For this reason, we will restrict the domain of the transformation to the set of points lying outside of the circle of unit radius centered at (0,0).

In order to better understand the Joukowski transformation, let us first consider the transform of a circle in the $\zeta-plane$ parametrized as $\zeta = re^{i\theta}$. From Eq.(2.4) we have

$$z = \left(r + \frac{1}{r}\right)\cos\theta + i\left(r - \frac{1}{r}\right).\sin\theta \tag{2.5}$$

When $r > 1$ an ellipse with principal axes $r \pm a^2/r$ is described in the $z-plane$. Looking at *Figure 2.4* one can see how the ellipses grow filling the hole plane, where the exterior of

the ellipses correspond to the exterior of the circles. For higher radius of the original circle, the ellipses grow until they also correspond to a circle in the new plane. Circles of smaller radii come closer to the poles located at $\zeta = \pm 1$, and therefore are more strongly affected.

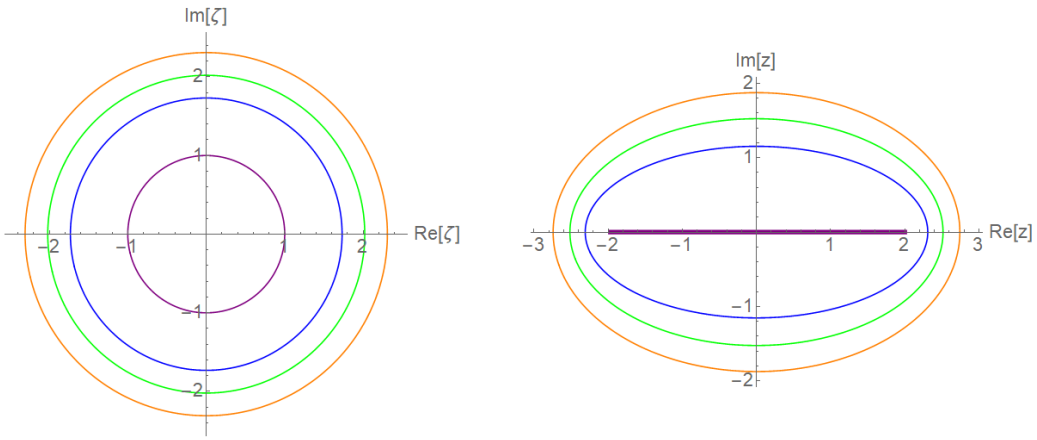

Figure 2.4: Circles of $\zeta = re^{i\theta}$ (left panel) under the Joukowski transformation in $z-plane$ (right panel).

The most interesting case is the purple circle crossing through the poles mentioned above at $\zeta = \pm 1$, here the Joukowski transformation generates a line segment of length $l = 4a$ in the $z-plane$. This line segment going from $-2a$ to $2a$ can be used in order to analyze the case of potential flow around a flat plate of finite length, which will be discussed in *Section 3.2.*.

One of the greatest advantages of the Joukowski transform is that under specific conditions they map circles into a variety of airfoils. An airfoil is generated whenever the input circle intersects one and only one of the two poles, and it has radius larger than 1. This can be done by considering circles generated by $\zeta = r_p e^{i\theta} - z_p$, with $\mathrm{Re}[z_p] < 0$ and $r_p = \sqrt{|1 - z_p|^2}$. As can be seen in *Figure 4.7*, by moving the center of the circles to the negative side of the real axis and expanding the imaginary part, the airfoil changes from a symmetric airfoil to a more curved profile.

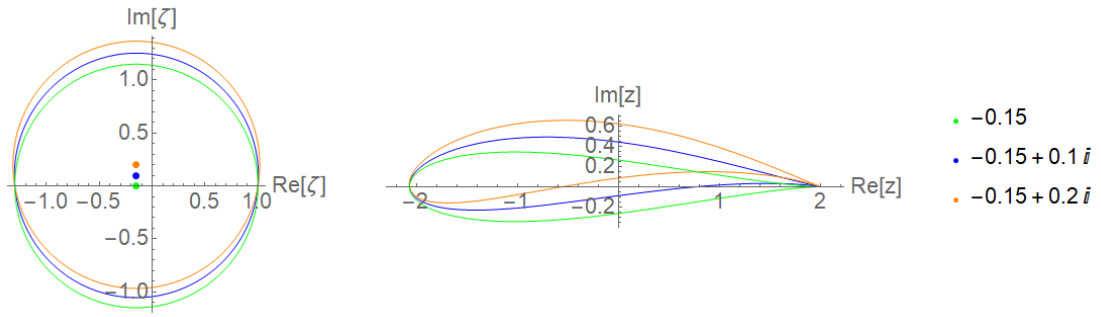

Figure 2.5: Initial circles (left panel), Joukowski airfoil transforms (right panel).

In order to plot the potential flows in the $z-plane$, the Joukowski transform has to be inverted from (2.4) to obtain ζ as function of z,

$$\zeta = \frac{1}{2}\left(z \pm \sqrt{r_1 r_2}\, e^{i(\theta_1+\theta_2)/2}\right), \tag{2.6}$$

where the necessary lengths and angles are taken from *Figure 2.6* (obtained from [4]).

This last equation will be the one used in the complex potentials to transform the original potential into the desired one just by replacing the parameter z by ζ in the equation (deeply explained in *Chapter 3*).

The segment going from $-2a$ to $2a$ is the branch cut mentioned above. A branch cut is a line in the complex plane across which an analytic multivalued function becomes discontinuous. For convenience branch cuts are often taken as straight lines or segments (as in the case of study). Knowing this, the analytic solution found for the potential flows across this segment of the space will not be reliable and should be discarded.

$r_1 = |z-2a|$

$r_2 = |z+2a|$

$\theta_1 = \arg(z-2a)$

$\theta_2 = \arg(z+2a)$

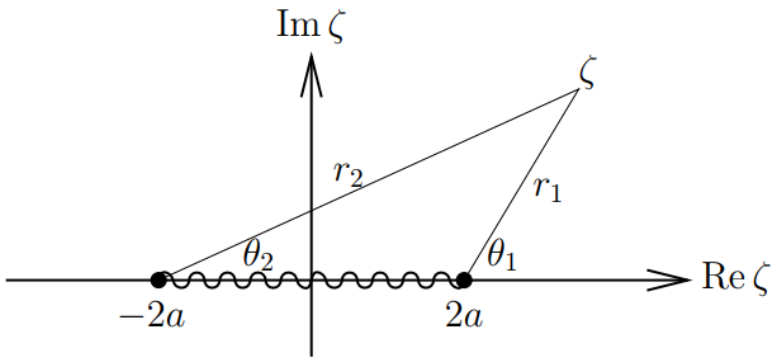

Figure 2.6: Graphical definition of r_1, r_2, θ_1 and θ_2

CHAPTER 3. JOUKOWSKI TRANSFORM APPLICATION

The main objective of this research is to achieve the representation and posterior analysis of perfect fluids patterns on different surfaces and configurations. To do so, it was decided that the most interesting strategy was to drive the analysis in an analytic way with the aim of finding accurate results, similar to that made by advanced softwares based on numerical methods (e.g. Ansys Software). Given that the theoretical equations have already been described in the theory of complex potentials 1.3., now it will only be necessary to describe the stream function and potential equations that correspond to each case.

3.1. Basic flow patterns

First of all, it is exposed the definition of basic flow patterns needed to achieve more complex and thus more interesting configurations. Even though there are four patterns that are normally considered basic, for the objectives of the present work we focus on the uniform and doublet flow.

3.1.1. Uniform flow

A flow with free stream velocity U along the direction α from the horizontal axis may be described by the complex potential

$$F(z) = i\,U\,\frac{z}{e^{i\alpha}} \tag{3.1}$$

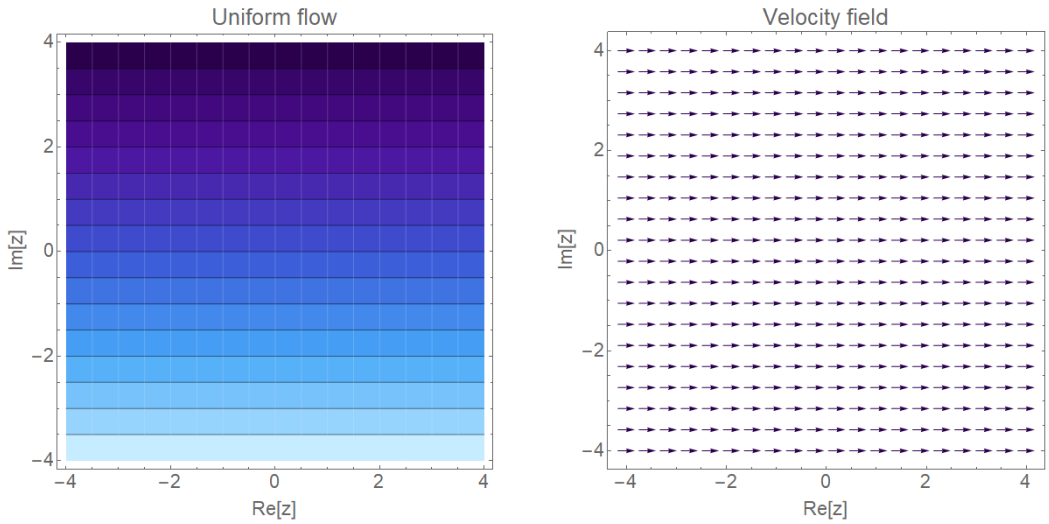

Figure 3.1: Uniform flow pattern for $\alpha = 0$. Left panel: stream lines in black lines, velocity potential in white lines. Right panel: Velocity field generated

In the left panel of *Figure 3.1* it is shown how the streamlines represented by black lines go straight and parallel horizontally and also the iso-contours of the velocity potential in white color perpendicular to streamlines. On the right panel it can be seen the field of the constant valued free stream velocity U that has been computed by differentiating the complex potential in *Eq.* (3.1), as discussed in *Eq.* (1.12).

The different colors represent different magnitudes of the stream function. The important part of stream function representation is not its value but the streamlines configuration on the plane.

3.1.2. Doublet flow

The second interesting case deals with the doublet flow that can be interpreted as the combination of a source-sink pair of infinite strength kept an infinitesimally small distance apart. The complex potential of strength k generated is

$$F(z) = i\,\frac{k}{2\pi}\frac{1}{z} \tag{3.2}$$

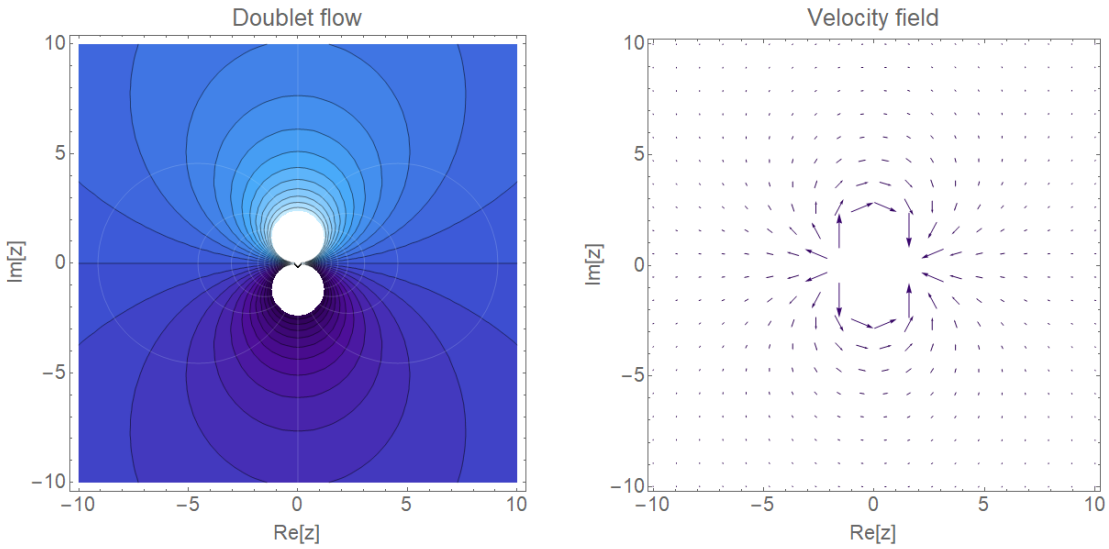

Figure 3.2: Doublet flow pattern. Left panel: stream lines in black lines, velocity potential in white lines. Right panel: Velocity field generated

Now, the streamlines are tangent to real-axis and flow counter-clockwise in the lower-plane and clockwise in the upper-plane. The reason why the potential is white at the centres is because it is proportional to $1/r$ thus when $r \to 0$ the function goes to infinite and it is not represented, see *Figure 3.2*.

The rotation sense can be seen in the velocity field shown on the right panel of *Figure 3.2*, far away from the doublet the flow slows down and has nearly zero velocity. This may be caused by the combination of the source-sink at the center, far away the effects are not so remarkable.

3.1.3. Flow around a circular cylinder

It is time to develop fluid equations around a circular cylinder. This case is one of the most important in this research since it will be the initial case to transform. Joukowski transformation will carry out the mapping from the circular cylinder to the airfoil profile in order to analyze fluid flow around it.

The classical example when trying to understand potential flows is the transverse flow crossing a circular cylinder. This configuration can be achieved by joining the uniform and doublet flows, given that when one has nearly zero velocity the other remains constant and results on a very smart combination. The complex potential F and the velocity field $\vec{v}$ for flow around a cylinder of radius R are

$$F(z) = i\,U\left(\frac{z}{e^{i\alpha}} + \frac{R^2\,e^{i\alpha}}{z}\right) \qquad v_y + iv_x = i\,U\left(e^{-i\alpha} - \frac{R^2\,e^{i\alpha}}{z^2}\right) \tag{3.3}$$

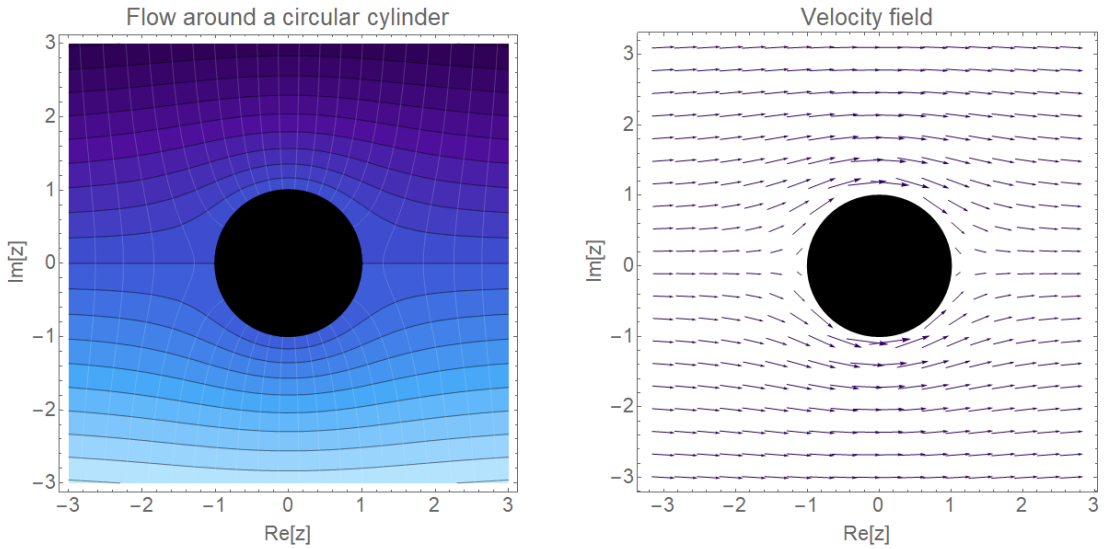

Figure 3.3: Left: stream function (black lines) and velocity potential (white lines) around a cylinder of unit radius. Right: velocity field.

Figure 3.3 shows how in this case the streamlines surround the cylinder without creating any turbulence or dispersion in the flow. Lines are shorter upstream, signaling a deceleration from the free velocity U. Looking at the streamline in the real-axis it is possible to see how it is divided when it touches the cylinder perpendicularly, this point is called stagnation point, where the local velocity is zero and the static pressure is maximum.

Shown in the velocity field distribution, the free velocity U will again appear after the second stagnation point on the real axis once the cylinder has been crossed. Above and below the cylinder the field is completely symmetric so there is no ascending force appearing on the surface. The flow would just cross and return to uniform configuration.

3.2. Joukowski transform application on complex potentials

As has been developed in *Section 2.3.*, the method consist on finding a solvable problem that is completely understood in the original plane, and then, mapped through the Joukowski transform. The final result is exact, and may therefore for example be used to test the accuracy of CFD simulations.

Beginning by the reproduction of the flow around an ellipse and passing through the flat plate and symmetrical wings, the complexity will be increased until reaching an airfoil profile with variable curvature and chord.

3.2.1. Ellipse

To a very rough degree, an airfoil may be approximated by an ellipse. The difference between the circular profile (see Section 3.1.3.) and the ellipse lies on the new length of the radius, which now it is not constant so the surface is flattened on the upper and lower part.

The mapping will be developed by the holomorphic function ζ defined in *Eq.* (2.6) applied on the complex potential describing the flow around a circular cylinder $W(\zeta)$

$$W(\zeta) = i\,U\left(\frac{\zeta}{e^{i\alpha}} + \frac{R^2\,e^{i\alpha}}{\zeta}\right) \tag{3.4}$$

The key point of the transformation comes when defining the value of R. For an ellipse to be created, this parameter has to get a value bigger than one, $R > 1$ ($R = 1.5$ in this case). With this assumption and for an angle of attack of 10°, the result is plotted in *Figure 3.4*.

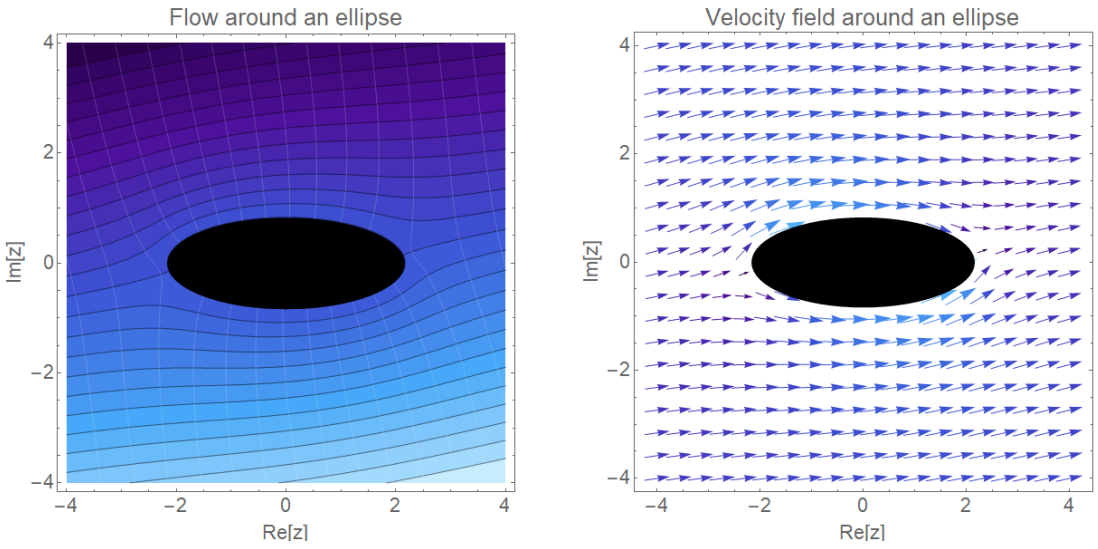

Figure 3.4: Flow around an ellipse at $\alpha = 10^o$. Left panel: stream function (black lines) and velocity potential (white lines). Right: velocity field.

As can be seen in *Figure 3.4* the flow around the ellipse is similar to the one around the cylinder (see Fig. 3.3) but now the flow does not cross the body symmetrically. Also the

velocity field is very similar to the circular cylinder with two stagnation points, one in the lower left part and the other on the upper right part of the surface.

3.2.2. Flat plate

Flat plates were the first to be discovered to create an ascending force when crossing through a fluid with a certain angle of attack. Thus, they are a fundamental shape to analyze for the research.

Once again, the most important parameter when carrying out the mapping is the value of R that has to be set so that the initial circle before the transformation crosses through the poles at $\zeta = \pm 1$ degenerating into a flat plate going from -2 to $+2$.

The function $\zeta = g(z)$ is the same as in the previous *Section 3.2.1.*, always with $a = 1$, but the complex potential is now

$$W(\zeta) = i\,U\left(\frac{\zeta}{e^{i\alpha}} + \frac{e^{i\alpha}}{\zeta}\right) \tag{3.5}$$

First, it should be analyzed the case of a flat plate that is located in the same direction as the fluid flows. The expected situation is that the flow remains unaltered due to the fact that the plate is infinitesimally thin.

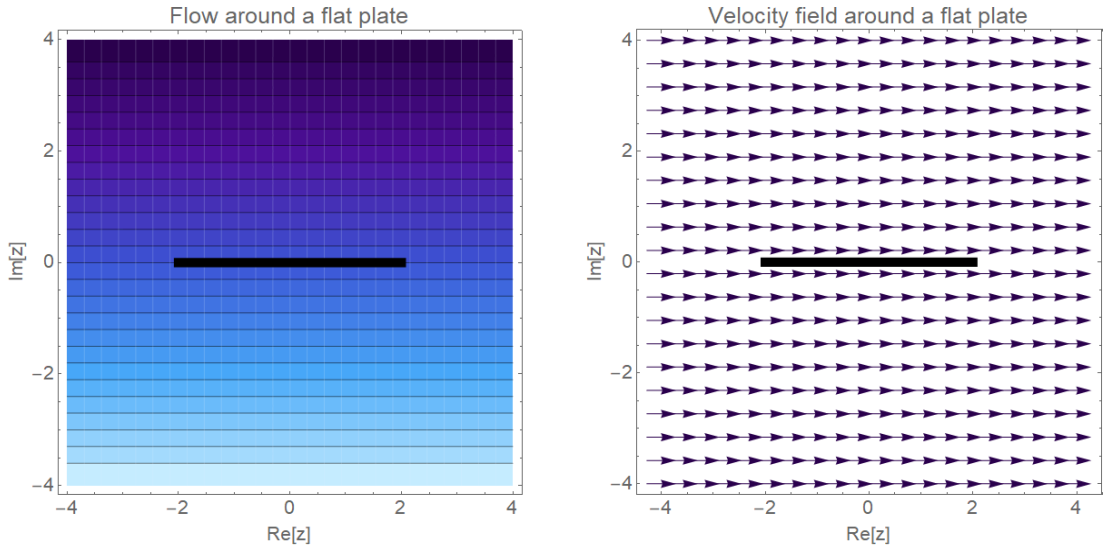

Figure 3.5: Flow around a flat plate at $\alpha = 0^o$. Left: stream function (black lines) and velocity potential (white lines) around a flat plate. Right: velocity field.

It can be seen in *Figure 3.5* how the stream lines cross straight without any perturbation. Also in the right panel of the figure, the arrows of the velocity field point to the right exactly as in the case of the Uniform Flow (*Section 3.1*).

The situation becomes more interesting to be analyzed when the flow crosses around a flat plate within a certain angle of attack α. The complex potential in that case will be affected by the $e^{i\alpha}$ term, which had previously been reduced to 1 and therefore did not affect the function.

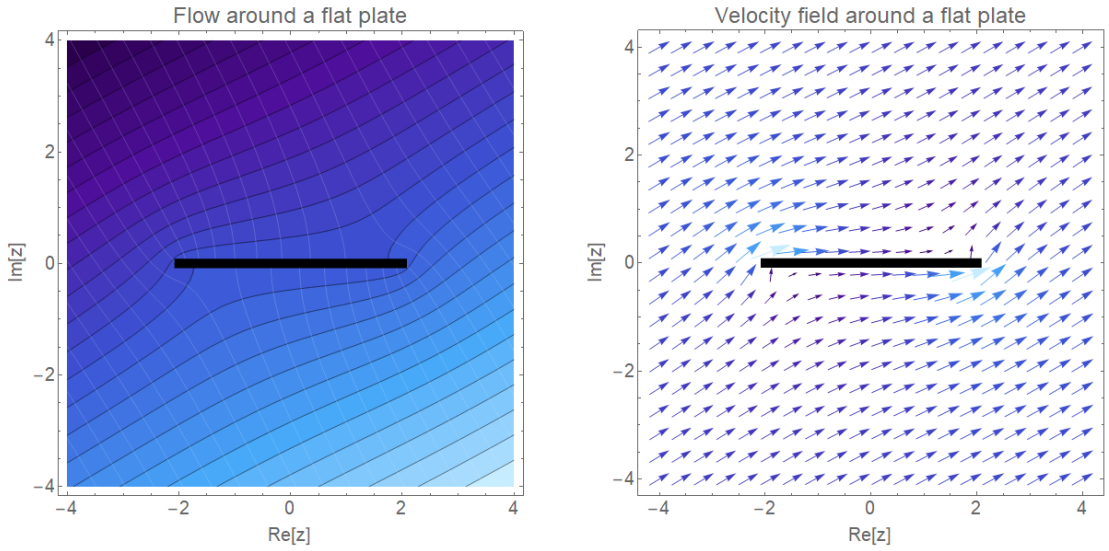

Figure 3.6: Flow around a flat plate at $\alpha = 25^o$. Left: stream function (black lines) and velocity potential (white lines) around an inclined flat plate. Right: velocity field.

In *Figure 3.6* the two points where the local velocity is zero (thus the pressure is maximum) are now located one in the upper and one in the lower part of the plate. Naively, one would think that with this angle of attack the plate should have to create an ascending force but this is not true with this configuration. For the flat plate to create lift, as we will see in the next Chapter 4 some condition (related with circulation) should be applied so that the flow on the upper part of the surface travels faster than the lower.

3.2.3. Airfoil

Airfoil design is normally divided in direct (evaluates a given shape and modifies it to improve the performance) and inverse (target a pressure distribution) methods. In this research, the main objective is to analyze the effects occurring on the flow by the airfoil, not to find the best profile. Once this is clarified, it should be well defined the method used because it is none of the above.

First of all, the Joukowski transformation center is determined. As has been stated before (see *Section 2.3.*), for an airfoil to be created it is necessary to place the center of the original circle in the left half of the complex plane. For a symmetric airfoil the imaginary part has to be zero, while non-zero imaginary values give a certain cusp.

The complex potential is once again the one used for the original cylinder but this time the transformed circle is centered in z_p (with $\mathrm{Re}[z_p] < 0$) and it has radius $r_p = \sqrt{|1 - z_p|^2}$

$$W(\zeta) = i\,U\left(\frac{\zeta - \zeta_p}{e^{i\alpha}} + \frac{r_p\, e^{i\alpha}}{\zeta - \zeta_p}\right) \tag{3.6}$$

When the flow crosses around an airfoil with null angle of attack, what is expected is that the flow remains unaltered far away from the surface. Looking at *Figure 3.7* it can be seen how this prediction is achieved.

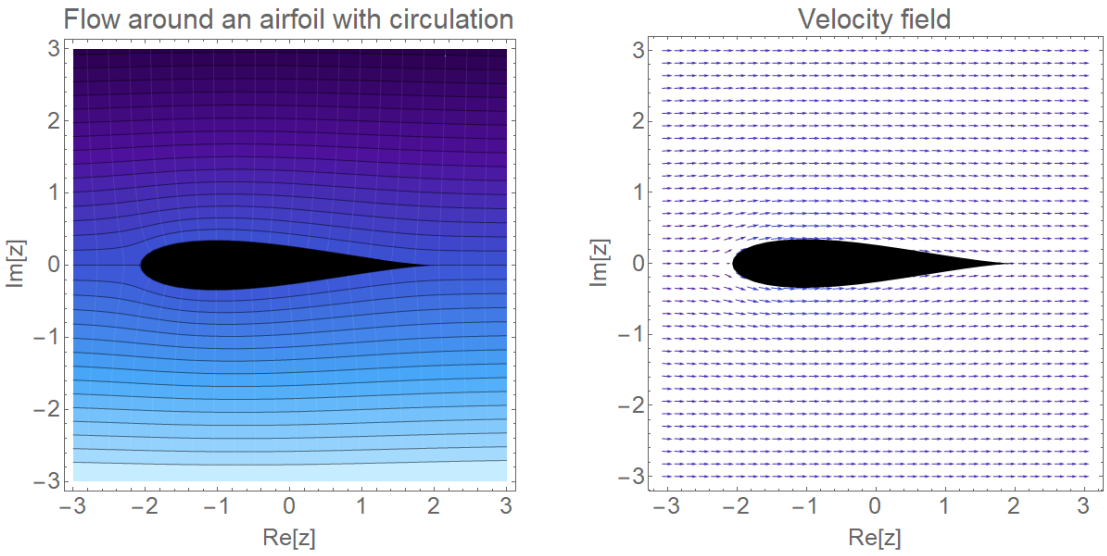

Figure 3.7: Flow around a symmetric airfoil at $\alpha = 0^o$. Left: stream function (black lines) and velocity potential (white lines) around an airfoil. Right: velocity field.

The stream lines surround the airfoil softly locating the stagnation points one at the leading edge and one at the trailing edge. In both the pressure would be higher than in any other point of the field.

The objective of having an airfoil with some angle of attack with respect to the flow is to create an ascending force that sustains the aircraft porting this airfoil.

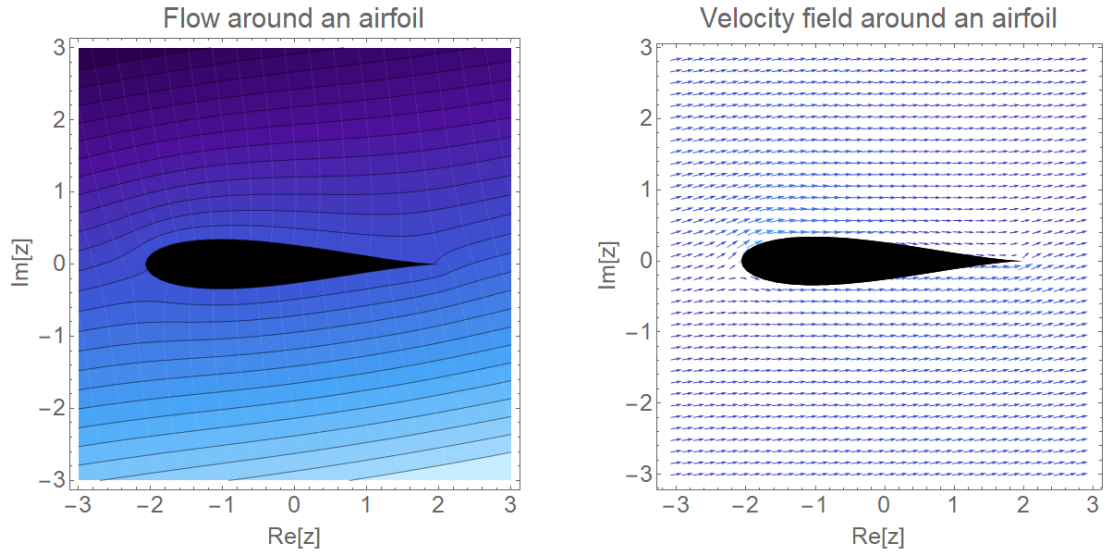

Figure 3.8: Flow around a symmetric airfoil at $\alpha = 10^o$. Left: stream function (black lines) and velocity potential (white lines) around an airfoil. Right: velocity field.

The results corresponding to an airfoil with an angle of attack of 10^o shown in *Figure 4.6* it can easily be seen how the flow far away from the surface remains unaltered. Furthermore, the velocity on the extrados does not increment more than the one on the lower part. For that to happen, thus for lift to be created, circulation has to be taken into account.

As will be seen, there exists a value of circulation Γ for which the stagnation point is displaced to the trailing edge so the velocity at this point is zero. With that, Kutta Condition is achieved and a more realistic situation is represented with the flow not remaining unaltered.

CHAPTER 4. KUTTA-JOUKOWSKI LIFT THEOREM

Kutta-Joukowski Lift Theorem gives the relation between circulation and lift on a rigid body with sharp corners (such as trailing edges of airfoils) moving at a constant speed in steady uniform flow conditions. The drag force experienced by the body would be parallel to the flow while the lift force would be perpendicular to the flow at every point.[6]

Jean le Rond D'Alembert modeled mathematically the effects produced by an incompressible and inviscid potential flow around a rigid body, getting as a conclusion that the drag force, D, experienced by the body was equal to zero and the lift force, L, was the only affecting the body as it is stated in

$$D - iL = i\rho U\Gamma, \tag{4.1}$$

where U is the free stream velocity, L is the lift force, ρ is the density of the fluid and Γ stands for the circulation (explained in *Section 4.1.*).

Kuethe and Schetzer state the Kutta condition as follows:[8]

> " A body with a sharp trailing edge which is moving through a fluid will create about itself a circulation of sufficient strength to hold the rear stagnation point at the trailing edge."

When using Kutta-Joukowski Theorem to calculate the lift created by an airfoil the Kutta condition becomes very significant due to the stagnation point placement on the trailing edge that generates a finite circulation of air around the airfoil. With zero-lift flow, the stagnation point lies on the upper trailing edge of the airfoil, while with the Kutta condition the stagnation point drops towards the trailing edge.

Figure 4.1 shows the displacement of the stagnation point that generates the circulation creating the lift force. On the upper figure, the situation shows a zero-lift flow with the stagnation point on the upper trailing edge. In this case, the velocity from the upper and lower part of the airfoil cross in the trailing edge, while on the bottom one, the Kutta condition is established, the stagnation point lies on the trailing edge and the velocity flows parallel.

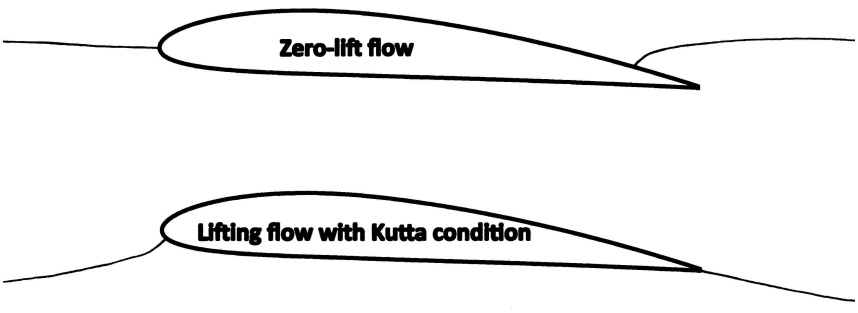

Figure 4.1: Stagnation point placement under Kutta condition.

Whenever the speed or angle of attack of an airfoil changes there is a weak starting vortex which begins to form normally above the trailing edge. This weak starting vortex causes the Kutta condition to be re-established for the new speed or angle of attack. As a result, the circulation around the airfoil changes and so too does the lift in response to the changed speed or angle of attack.[14]

4.1. Circulation and Kutta condition application

Circulation represents how much a flow rotates along a contour. It is often used in fluid dynamics as an intermediate variable used to calculate the forces acting on a body. In this case, it will be the parameter that will cause the reestablishment of the stagnation point position over the airfoil surface. Represented by Γ, it can be applied in complex potentials as a vortex rotating in the desired direction (positive for counter-clockwise, negative for clockwise). To do so, the function $F(z)$ should be defined as

$$F(z) = \frac{\Gamma}{2\pi}\log(z) = \frac{\Gamma}{2\pi}[\log(\rho) + i\theta] \tag{4.2}$$

From $F(z)$, the velocity field can be obtained deriving the previous equation as

$$\frac{\mathrm{d}F}{\mathrm{d}z} = \frac{\Gamma}{2\pi}\frac{1}{z} \tag{4.3}$$

Since the latter complex potential is an analytic function, it may be added to other complex potentials to obtain more complex flow patterns.

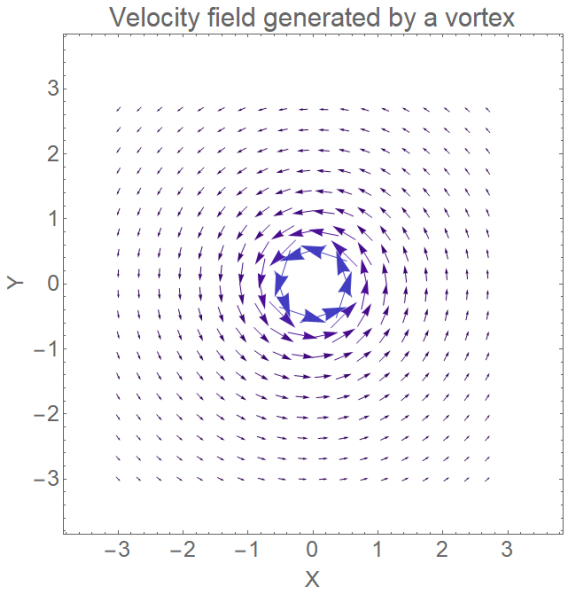

Figure 4.2: Velocity field generated by a single vortex located at the origin of the $z - plane$.

Vortices will be necessary to apply Kutta condition as the value of the circulation created by that vortex will determine if the rear stagnation point is located at the trailing edge or not.

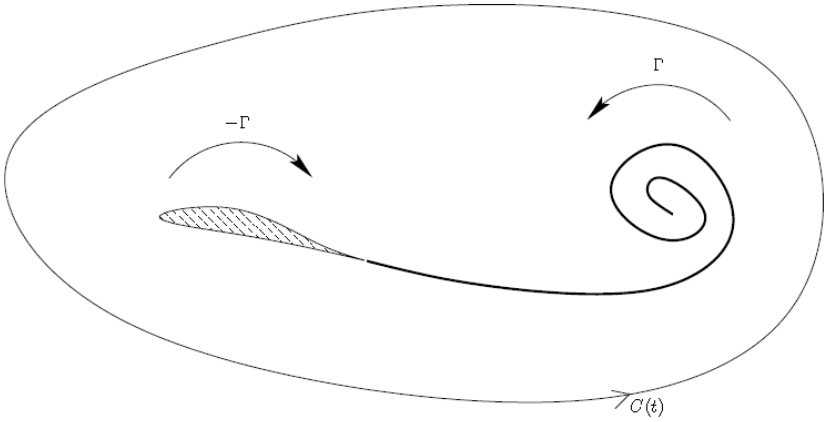

Figure 4.3: Schematic of a trailing vortex behind an airfoil. The material curve $C(t)$ encloses both the vortex and the airfoil. (Picture from [4])

Kelvin's Circulation Theorem states:[11]

> "In a barotropic ideal fluid with conservative body forces, the circulation around a closed curve (which encloses the same fluid elements) moving with the fluid remains constant with time."

Figure 4.3 shows how when a body begins to fly, it generates a starting vortex behind it that would invalidate Kelvin's Theorem. For that not to happen, an equal and opposite circulation around the surface must be created so that the theorem is still true over a large contour $C(t)$.

In numerical simulations, in order to apply Kutta condition on a mesh, it would just be necessary to introduce new conditions to the points situated on the trailing edge of the airfoil. However, in the case of study, there is no mesh so the problem has to be solved analytically.

First of all, as an approach it is studied the case of the flow around a circular cylinder with some circulation applied so that the velocity field is changed and lift force is created. This case is known as Magnus effect (see [15]).

For the case of study, the velocity field without circulation is defined as

$$v_{cyl} = i\,U\left(e^{-i\alpha} - \frac{R^2 e^{i\alpha}}{z^2}\right) \tag{4.4}$$

In this equation circulation is not affecting the velocity field so Kutta condition cannot be met. For that to happen, the vortex velocity equation explained right above has to be added

$$v'_{cyl} = i\,U\left(e^{-i\alpha} - \frac{R^2 e^{i\alpha}}{z^2}\right) + \frac{\Gamma}{2\,\pi\,z} \tag{4.5}$$

Knowing the velocity field around a rotating circular cylinder, it is just necessary to equal *Eq.* (4.5) to zero, given that stagnation points are those where the local velocity vanishes.

This procedure yields the stagnation points

$$z = i\,R\,e^{i(\alpha\pm\varphi)}, \tag{4.6}$$

where $\varphi \equiv \arccos[\Gamma/(4\pi RU)]$.

Changing the circulation will affect the location of the stagnation points; for example, to have a stagnation point located at the point $z = R + 0i$, one needs to impose a circulation

$$\Gamma = -4\,\pi\,R\,U\sin\alpha. \tag{4.7}$$

With this procedure, it has been achieved an expression not only for the stagnation points but also for the circulation value created for a specific angle of attack α. This circulation equation of three degrees of freedom (R, U, α) would completely be defined with the inputs given in the beginning of the simulation.

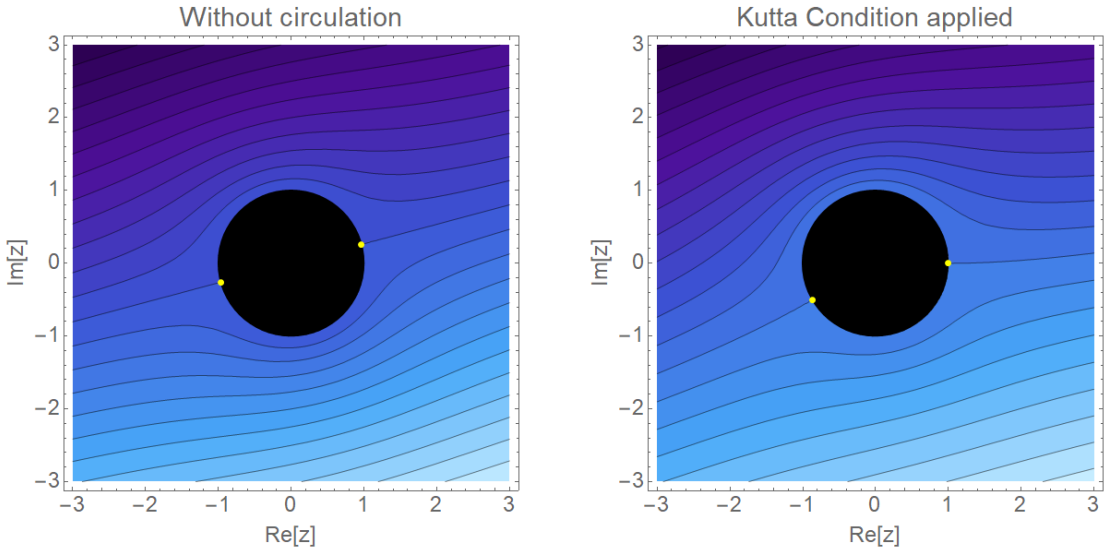

Figure 4.4: Adding circulation around a circular cylinder with a flow at $\alpha = 15^o$. Yellow points show the stagnation points. Left panel: fluid behaviour without circulation. Right panel: fluid behaviour with circulation chosen such that one of the stagnation points lies at $z = R + 0i$.

It can be seen in *Figure 4.4* how for $\alpha = 15^o$ and no circulation the streamlines are equal in the upper and under part of the cylinder. When a circulation is created around the cylinder, the streamlines narrow at the top and widen at the bottom what means that the velocity is bigger up and thus lift force is created upwards. As shown with yellow points, the stagnation points now are located a bit downward.

Once achieved the representation of the stagnation points on a circular cylinder, the next step is to apply Joukowski transform to get those points to match with the trailing edge of the wing. In this case, as the trailing edge is always located at $2a$ the condition that has to be fulfilled is that the right stagnation point has null imaginary part

$$\mathrm{Im}[z + \frac{1}{z}] = 0, \tag{4.8}$$

which yields the stagnation points in the $z - plane$

$$z = z_p + i\,R_p\,e^{i(\alpha\pm\varphi)}. \tag{4.9}$$

Here φ has the same value as for the cylinder and the circulation is now

$$\Gamma = -4\,\pi\,R_p\,U\sin\alpha + \frac{\mathrm{Im}[z_p]}{R_p} \tag{4.10}$$

Once again, the deterministic parameter is the angle of attack that generates the value of the circulation and thus the lift force. What is expected to happen is that the point drops to the trailing edge fulfilling then the Kutta Condition.

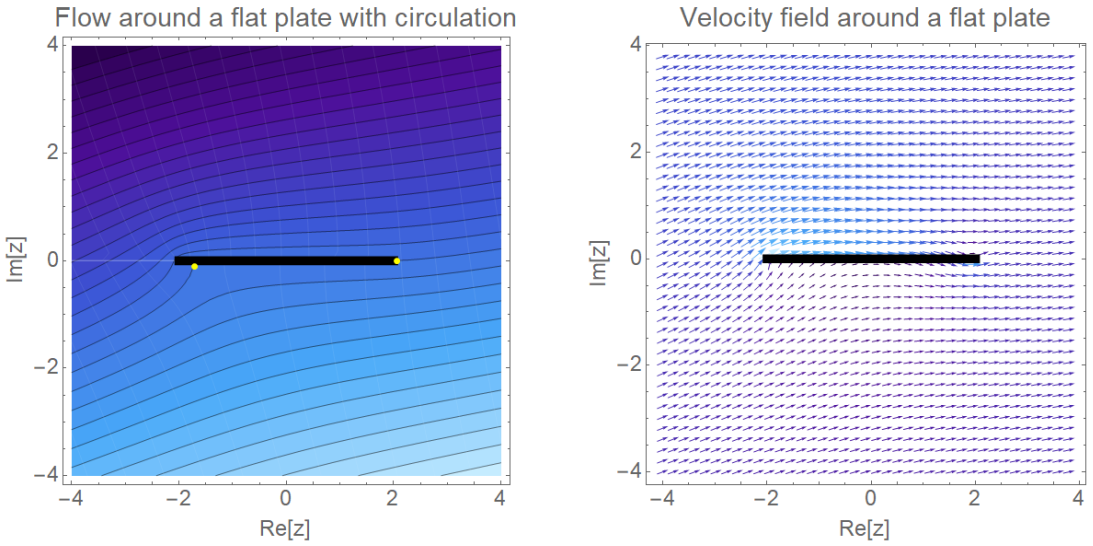

Figure 4.5: Application of Kutta condition in a flat plate at $\alpha = 15^o$. Left panel: Stream function. Right panel: Velocity field. Yellow points show stagnation points location.

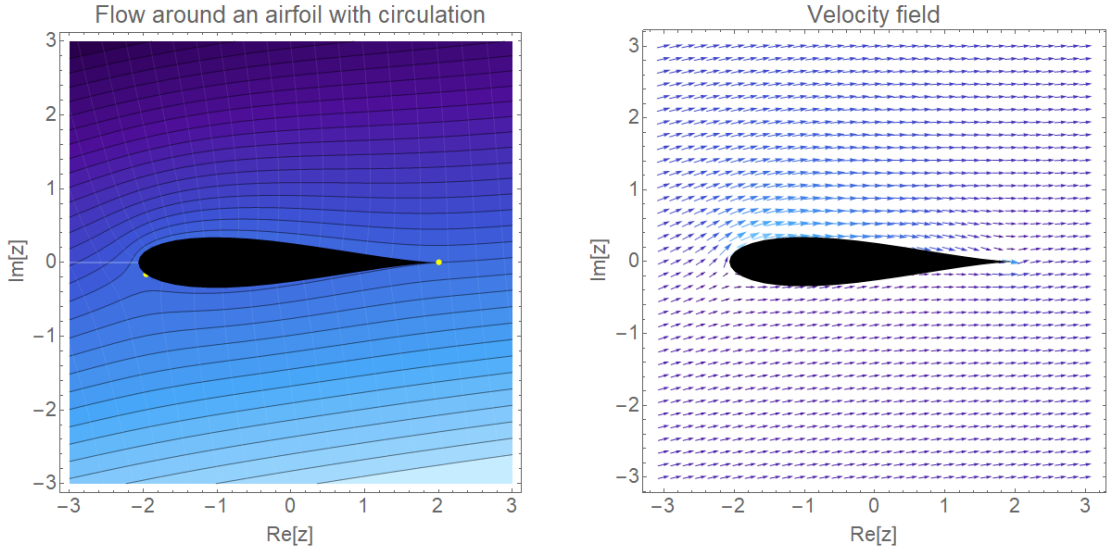

Figure 4.6: Application of Kutta condition on a symmetric airfoil at $\alpha = 10^o$. Left panel: Stream function. Right panel: Velocity field. Yellow points show stagnation points location.

As it is shown in *Figure 4.5* and *4.6*, the formulation made in this section correctly achieves the representation of the real situation of a perfect fluid crossing a flat plate and an airfoil.

The stream lines enter with the selected angle of attack, surround the surface and leave parallel to the end point of the profile in a smooth manner.

It can be more clearly seen both in *Figure 4.5* and *4.6* (right panel) how the velocity field surrounding the surfaces exits parallel, and not at an angle as happened before.

Different profiles have been shown to comply with the Kutta condition showing consistent results, which leads us to think once again that this could be a very interesting method as a first approach to the design of wings. Always bearing in mind that the branch cut is under the airfoil so that it does not affect to the flow representation.

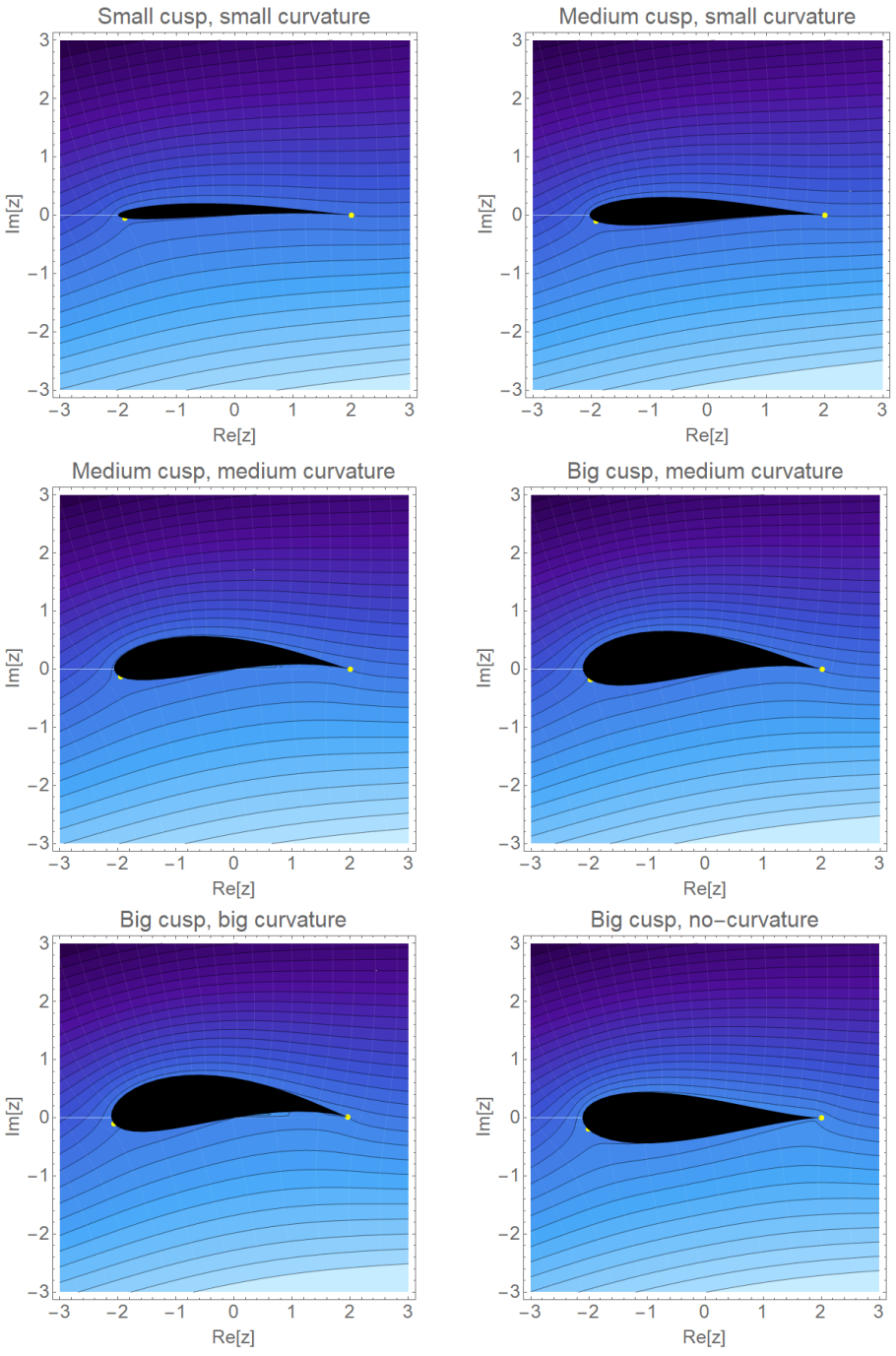

Figure 4.7: Study of different airfoils at $\alpha = 10^o$.

4.2. Pressure distribution and lift calculation

Once Kutta condition has been applied, it would just be necessary to make one more step to get the pressure distribution and the lift generated by these surfaces.

In order to get the actual pressure on the surface of the airfoil, it is necessary to apply Bernoulli's equation which says that increasing the velocity decreases the local pressure, and vice-versa. [17]

$$p - p_\infty = \frac{\rho}{2} U^2 \left(1 - \left(\frac{v}{U}\right)^2\right) \tag{4.11}$$

Where p is the actual pressure on every point and p_∞ is the pressure far away from the airfoil.

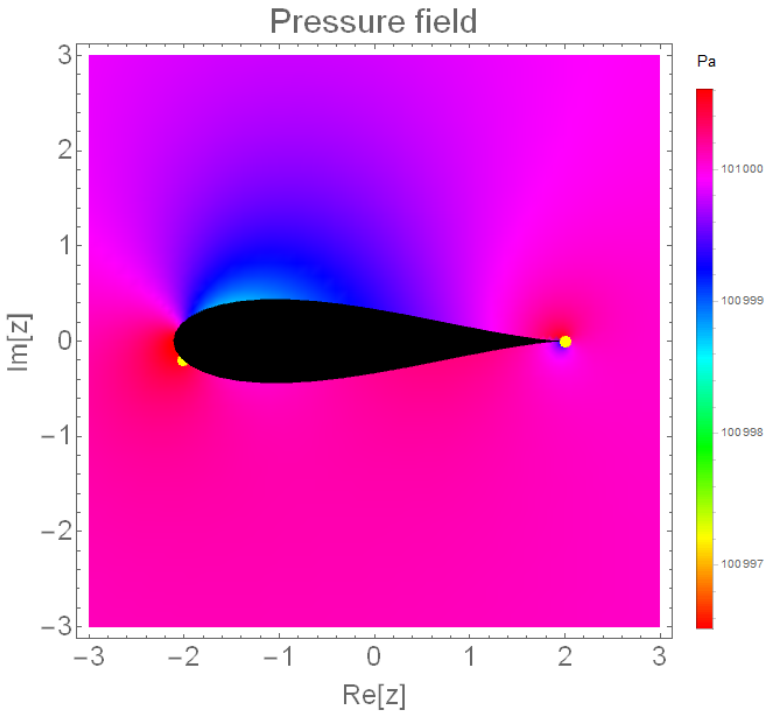

Figure 4.8: Actual pressure field generated by a symmetric airfoil at $\alpha = 10^o$

Figure 4.8 shows the absolute pressure generated around the symmetric profile with an angle of attack of $\alpha = 10^o$. Looking at the extrados it is easy to see that the actual value of the pressure is smaller than under the airfoil, if the pressure is smaller then it is again confirmed that the velocity is bigger and there exists an ascending force.

About the pressure on the stagnation points, the one on the leading edge is showing the highest possible value thus the smallest velocity. In the case of the trailing edge stagnation point on the lower part it shows discontinuous values that might be caused by the branch cut, although it is under the airfoil, the effects when applying the color of the plot might be latent.

For the lift, in this case it will be computed for the symmetric airfoil at 10^o of angle of attack shown in *Figure 4.6*.

It has already been explained that the drag force around a given body immersed in a perfect fluid was equal zero. In the case of lift force, it takes the leading role being completely defined by *Eq.* (4.1). Knowing the value of Γ, the equation would be

$$L = i\,\rho\,U^2\,4\,\pi\,R_p\left(\sin\alpha + \frac{\mathrm{Im}[z_p]}{R_p}\right) \tag{4.12}$$

For the symmetric airfoil of *Figure 4.6* in a standard atmosphere of $\rho = 1.225$ Kg/m3 and flying at $U = 50$ m/s it would generate a lift force of 7685.18 N.

CHAPTER 5. COMPLEX POTENTIALS ON NON-PLANAR SURFACES

Conformal mapping is not restricted to two-dimensions. This mathematical technique can also be used to transform a 2D plane into a non-planar surface embedded in 3D space. Since the combination of conformal maps is still a conformal map, a known flow solution on the plane (or a portion of it) can be used to derive the solution on a complex surface, to model for example airflow in the Earth atmosphere, or in front of the tip of a commercial aircraft (which often displays a hyperbolic shape).

In *Chapter 2* it was introduced a function $w = F(z)$ that transformed one complex plane into another

$$F(z) : \mathbb{C} \to \mathbb{C}$$

The objective now is to find a new function $S(z)$ that projects the primary plane into a non-planar surface in 3D:

$$S(z) : \mathbb{C} \to \mathbb{R}^3$$

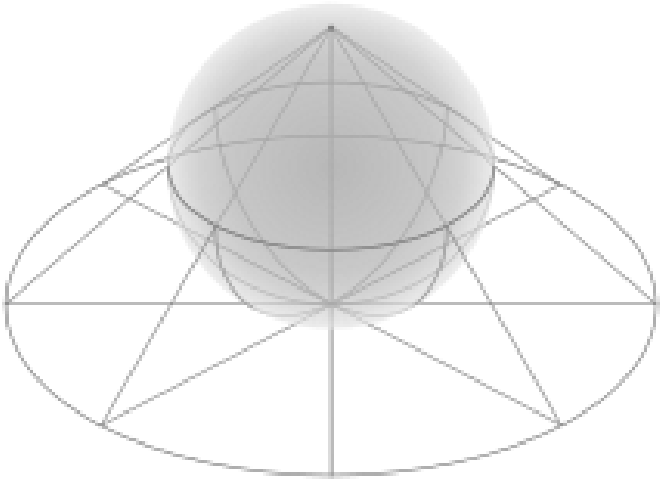

Figure 5.1: Stereographic projection from the North pole onto the plane. (from [16])

5.1. Spheres: Stereographic projection

Stereographic projection is a particular case of 3D conformal mapping $S(z) : \mathbb{C} \to \mathbb{R}^3$ that projects the complex plane onto a sphere of radius 1 (or viceversa). The transformation can be parametrically defined as

$$(x, y, h) = \frac{1}{1+z^2} \left(2\,\mathrm{Re}[z],\ 2\,\mathrm{Im}[z],\ -1+z^2 \right), \tag{5.1}$$

where $z = r\, e^{i\theta}$ is a complex number on the plane, and (x, y, h) are the coordinates of 3D space. This projection is defined on the entire sphere, except at the projection point (given that this point corresponds to a circle of infinite radius in the complex plane).

Once the projection equation has been defined, let us consider the case of a positive vortex located at the South pole of the sphere.

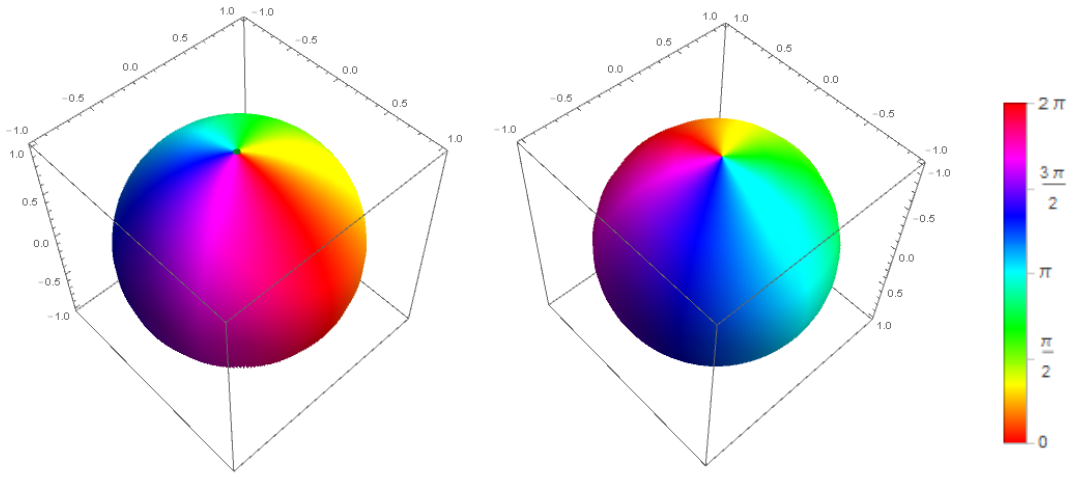

Figure 5.2: Phase of a vortex located on the complex plane at (0,0) projected onto a sphere.Left panel: Northern Hemisphere. Right panel: Southern Hemisphere.

Figure 5.2 shows the imaginary part of the complex potential of a vortex located at the South pole of the sphere. The imaginary part of *Eq.* (4.2) corresponds to the value of the phase.

Interestingly, the presence of a single vortex at the South pole (or at any other point of the plane) obligatorily generates another vortex, which appears here on the North pole (see the left panel of *Figure 5.2*). This is a consequence of a theorem, which states that the total charge (i.e., the sum of positive minus negative vortices) must always be zero on a compact surface. Let us note that, if one starts from a dipole on the plane, its total charge is directly zero, so that its projection on the sphere will not generate an extra vortex at the North pole. This is illustrated in *Figure 5.3*, where a configuration containing three dipoles is shown.

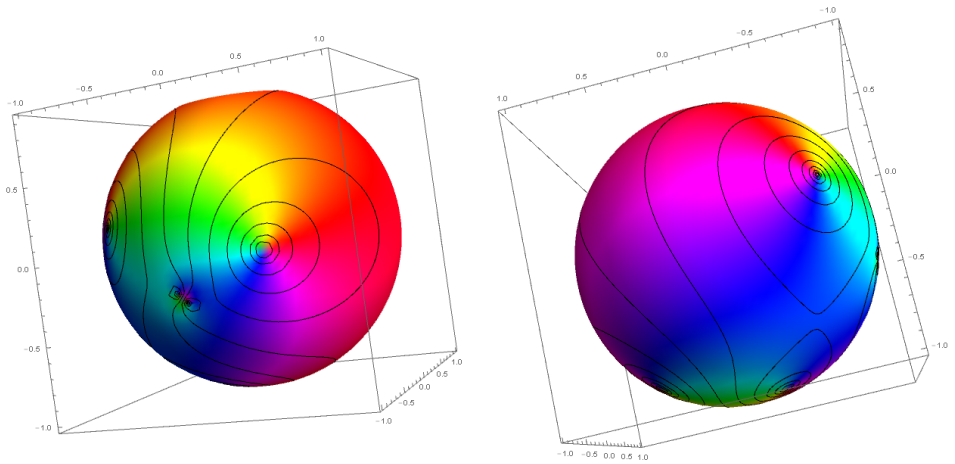

Figure 5.3: Flow distribution of three dipoles located randomly on the complex plane and projected onto a sphere. The black lines indicate the streamlines.

As stated just above, *Figure 5.3* shows three dipoles located over the surface of the sphere randomly. Constant color indicates same value of phase so it is indicating the distribution of the velocity potential. About the velocity field, knowing it is tangential to stream lines, it is possible to study the velocity direction by following the black lines of the figure. This method seems very powerful for meteorological purposes where there are cyclones (low-pressure, high-velocity areas) and anticyclones (high-pressure, low-velocity areas) that can be represented by vortices, and the wind surrounding them can be studied in order to make the weather predictions.

This short analysis demonstrates the great potential that it would have to represent vortices, sources or sinks (or any other complex potential) on the surface of a sphere. This could be a good method to study the winds even though other factors that can carry out a representation closer to reality should be taken into account.

5.2. Hyperboloids

Another interesting family of surfaces which may be considered is the one of hyperboloids. Hyperboloids often appear in the theory of special relativity, and a conformal map that generates them is called *Poincaré disk model* [18]. The latter maps the upper surface of the hyperboloid to a disk of unit radius, sending straight lines to segments of circles contained within that disk that are orthogonal to the boundary of the disk, as shown in *Figure 5.4*.

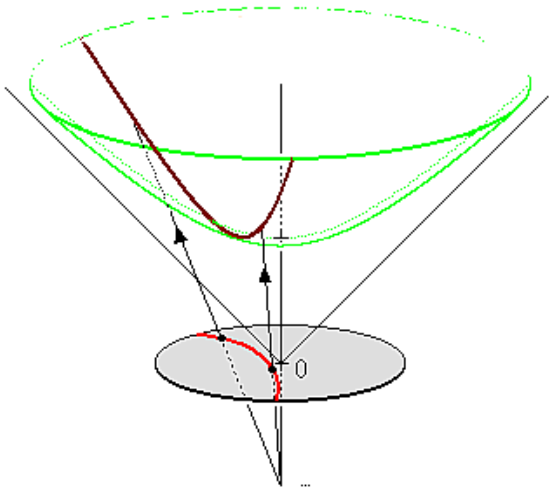

Figure 5.4: Hyperboloid projection from the Poincaré disk model. (Image from [19])

Hyperboloids are not equivalent to the whole complex plane, but only to a disk of finite radius. Therefore, to represent perfect fluid flow on such a surface it is first necessary to find the complex potential inside the disk, i.e., the one that satisfies the correct boundary condition, which require that the velocity is tangential to the disk. This task can be achieved simply by applying the *Method of Images* [20], a very useful tool for solving electrostatic and hydrodynamic problems, that solves for determinate boundary conditions by adding imaginary charges outside of the domain.

For the conformal disk model to be applicable it is necessary to fulfill the condition that the contours of a vortex (or whatever complex potential) located inside the disk are orthogonal to the boundary of the disk. *Figure 5.5* shows how the vortex inside the disk has its image outside achieving the contours of the complex potential created by both vortices to be orthogonal to the boundary of the disk. This configuration is achieved by using the complex potential

$$F(z) = \log(z - z_0) - \log(z - \frac{R^2}{\overline{z_0}}), \tag{5.2}$$

where $\overline{z_0}$ denotes the complex conjugate of z_0.

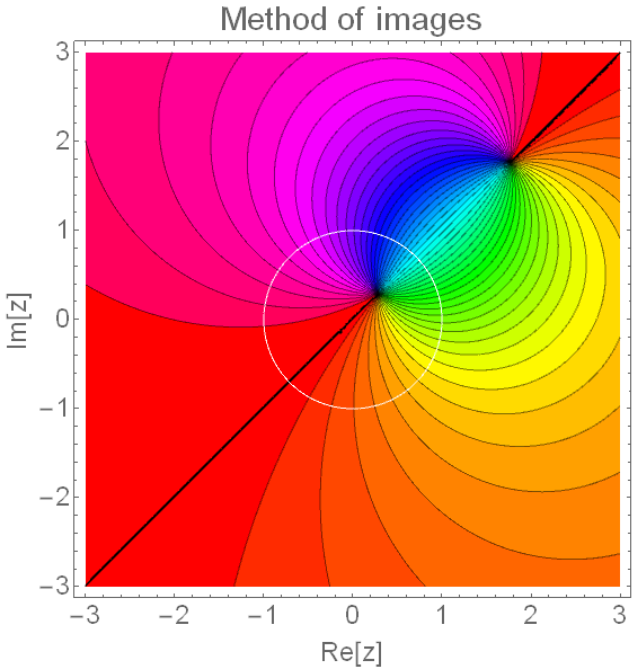

Figure 5.5: Vortex inside the unitary disk with its imaginary outside the disk.

The projection of the disk into a non-planar hyperboloid is then

$$(x, y, h) = \frac{1}{1 - z^2} \left(2\,\mathrm{Re}[z],\ 2\,\mathrm{Im}[z],\ 1 + z^2 \right). \tag{5.3}$$

An interesting application of hyperbolic conformal mapping is the possibility of studying the approximate behavior of the air when encountering the nose of a commercial aircraft or whatever surface with soft tip. For this purpose, it may be represented a source of fluid on the tip of the hyperbola, given that the air would encounter the surface and spread all over as happens in a source representation.

The complex potential defining the source at the center of the disk is simply

$$F(z) = i \log(z), \tag{5.4}$$

As shown in *Figure 5.6* the stream lines expand over the surface of the hyperboloid softly without intermixing. The velocity would do the same spreading backwards. For the case of the phase, it can be seen how it is bigger in the tip and then it becomes more or less constant.

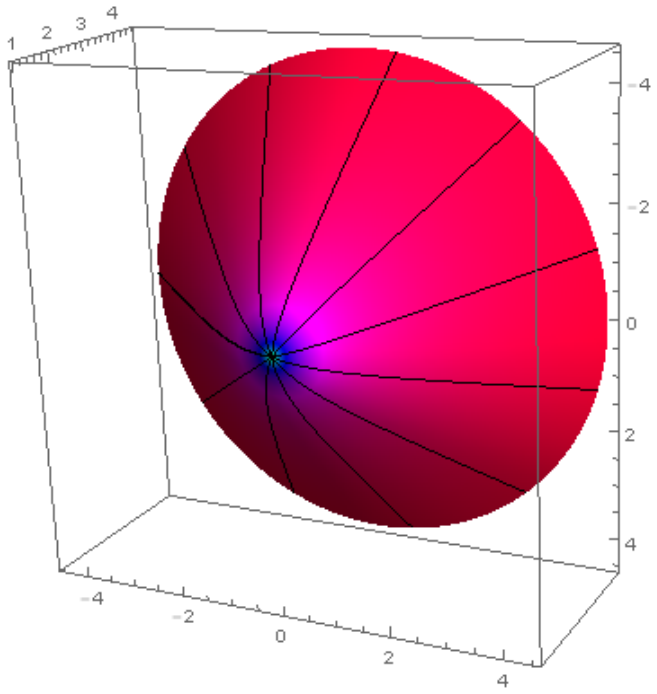

Figure 5.6: Flow distribution for a source located on the tip of an aircraft.

This is a new way to study the classical exercise that is normally raised in two-dimensions, i.e., on *page 596* of [10], where a fluid of velocity U encounters and surrounds a soft tip.

Non-planar mapping has resulted to be very useful when having complex surfaces where it is convenient to the study the effects of flow over the hole surface and not just on a section of it.

CONCLUSIONS

The main aims of this investigation were related to the study of fluid dynamics, which is a field of science that has already been studied on many occasions and of which there exist many written books.

The present document is the result of a different way to study perfect fluids, joining conformal maps with complex potentials to attack the problem in a completely analytic way, without grids, iterations or any other numerical procedure. Developing the investigation in this way has led to the need to pose a new thinking that had not been raised before in the degree. Analytic resolution of fluids flow has been achieved by developing a computer code that might be much more simple than the ones used for numerical calculations. In addition to that, the fact that the parameters are not iterated over and over leads to think that this would be an efficient way to achieve quite realistic results.

Chapter 3 has demonstrated that making a fluid flow analysis by using conformal mappings and complex potentials is perfectly achievable but it has not been until *Chapter 4* where consistent results have been represented. The fact of having introduced circulation around the surfaces has greatly increased the value of this method given that the reality is not far from the various figures obtained. From the uniform flow to the representation of vortices on the surface of non-planar spheres, this technique is applicable in as many cases as one can think of.

In the personal field, it has been a very enriching and rewarding experience being able to carry out this project. Even though this investigation might be more focused on a physical branch, it seems very important for an Aeronautical Engineer student to understand the behaviour of fluids even in very special cases such as perfect fluid conditions, because without that, an aircraft would not be able to fly. In addition to that, the fact of having to learn a new programming language has been a challenge since this field has always been a personal weak point but *Mathematica* has resulted to be a software with many powerful functions.

Future investigations could be carried out based on this document in all types of problems. In the design of wing profiles, for instance, it is usual to first make a preliminary approximation with the objective of knowing the approximate benefits that said profile could give. Here is where it could come this research, it has been demonstrated how powerful this technique is, thus it can be combined with numerical simulations to achieve even better results.

BIBLIOGRAPHY

[1] L. D. Landau and E. M. Lifshitz.*Fluid Mechanics. Second Edition*. (Institute of Physical Problems, USSR Academy of Sciences, Moscow. 2009) 5

[2] "How do molecules move in a liquid". (www.quora.com. July 2016) 5

[3] R. Feynman, R. Leighton, and M. Sands. *"The Feynman Lectures on Physics"*. (California Institute of Technology. 2013) 7

[4] "3 Conformal Mapping". *Part A. Fluid Dynamics and Waves*. (OCIAM Mathematical Institute, University of Oxford. February 2014) xi, 9, 11, 13, 25

[5] Water Environment Federation-American Water Works Association Joint Student Chapter. (University of Illinois at Urbana-Champaign. March 2018)

[6] "2 Two-dimensional incompressible irrotational flow". *Part A. Fluid Dynamics and Waves*. (OCIAM Mathematical Institute, University of Oxford. February 2014) 23

[7] "Analytic function". *General Complex Analysis*. (Wolfram, MathWorld. 2018) 11

[8] A.M. Kuethe and J.D. Schetzer (1959) Foundations of Aerodynamics, 2nd edition, John Wiley and Sons 23

[9] "What is the meaning of circulation found in Kutta condition?". *Aviation*. (Questions, Stack Exchange. January 2018)

[10] White, F.M. "Chapter 8. Potential Flow and Computational Fluid Dynamics"*Fluid Mechanics.*. (McGraw-Hill, New York, 1979) 35

[11] Kundu, P and Cohen. *1: Fluid Mechanics*. Page 130 (Academic Press 2002) 25

[12] Massignan, Pietro. "Superfluid vortex dynamics on peculiar surfaces". *UPC & ICFO*. (2017)

[13] https://es.wikipedia.org/wiki/Pierre-Simon_Laplace 7

[14] https://en.wikipedia.org/wiki/Kutta_condition 24

[15] https://en.wikipedia.org/wiki/Magnus_effect 25

[16] https://en.wikipedia.org/wiki/Stereographic_projection xii, 31

[17] https://en.wikipedia.org/wiki/Bernoulli%27s_principle 29

[18] https://en.wikipedia.org/wiki/Poincar%C3%A9_disk_model 33

[19] https://en.wikipedia.org/wiki/Hyperboloid_model xii, 33

[20] https://en.wikipedia.org/wiki/Method_of_image_charges 33